Perceptually Uniform Motion Space

Åsmund Birkeland, *Member, IEEE*, Cagatay Turkay, and Ivan Viola, *Member, IEEE Computer Society*

Abstract—Flow data is often visualized by animated particles inserted into a flow field. The velocity of a particle on the screen is typically linearly scaled by the velocities in the data. However, the perception of velocity magnitude in animated particles is not necessarily linear. We present a study on how different parameters affect relative motion perception. We have investigated the impact of four parameters. The parameters consist of speed multiplier, direction, contrast type and the global velocity scale. In addition, we investigated if multiple motion cues, and point distribution, affect the speed estimation. Several studies were executed to investigate the impact of each parameter. In the initial results, we noticed trends in *scale* and *multiplier*. Using the trends for the significant parameters, we designed a compensation model, which adjusts the particle speed to compensate for the effect of the parameters. We then performed a second study to investigate the performance of the compensation model. From the second study we detected a constant estimation error, which we adjusted for in the last study. In addition, we connect our work to established theories in psychophysics by comparing our model to a model based on Stevens' Power Law.

Index Terms—Motion visualization, motion perception, animation, evaluation, perceptual model

1 Introduction

The use of motion can be seen in visualization techniques frequently. It has various purposes, for instance depicting a data attribute, to attract attention, or to convey shape information. An advantage of using motion in visualization is that motion detection is a pre-attentive process in the human cognitive system [1]. Motion can then effectively guide the users' attention to interesting features in the data and reveal small details in the motion pattern [2].

Flow visualizations are aimed to provide insight into how a fluid deforms under applied shear stress for a given situation. Unlike data representing solid physical objects, there are no *real* structures in a flow apart from the different flow patterns. Still, when referring to the topology of a flow, there exist abstract structures such as critical points and vortices. While topology is an important aspect of flow analysis, the velocity magnitude is also important in many cases.

Another reason for deploying animation of particles in visualization is that this is often a direct visualization of a particular phenomenon and might be therefore appreciated by the domain specialist. It exhibits qualitative characteristics such as detailed flow behavior, similar to the real observable phenomenon. One example can be seen in simulation of flow around an airplane wing. The lift from a wing is generated from the low pressure over the wing caused by the difference in velocity of the air moving above and below the wing [3]. In medicine, blood-flow analysis is important in prevention, diagnosis, and follow-up monitoring of diseases. In this case, accurate flow data can be acquired with a range of techniques such as 4D Magnetic Resonance Imaging (MRI) for 3D flow, and B-flow ultrasound over time. For making correct decisions, multiple features of the flow have to be analyzed, such as pressure, vorticity and velocity.

Different visual cues can be utilized for different data attributes. Color coding is a typical method for depicting data. For instance, the velocity magnitudes in a flow field can be visualized with color. However, this provides no information regarding the direction of the flow, and other techniques such as glyphs must be applied in addition. The usage of color can be very efficient for a single data attribute. Still, there are other aspects of the flow that are often important for the user. An issue arises when more attributes should be visualized simultaneously. If color is already occupied for velocity magnitude, other means must be utilized.

In engineering, analyzing aerodynamics is often done by adding a flow of air around the object of interest. The air flow is as such not visible. To be able to actually see the flow, particles are added into the flow field. The motion of the particles conveys intuitively information regarding both the direction and the velocity magnitude of the flow. This technique has commonly been adopted into flow visualization [4], [5], [6], [7].

Investigations into how the human visual system processes motion can be approached from different directions. In the direction of neurophysiology, the fundamental laws of nature are applied for investigating the physical connection between motion detection and the neural activity. The approach is more directed towards signal processing, where one tries to understand how signals from the optic system are processed and transmitted into the visual cortex. This can be done either by applying physical models to simulate the neurological response in the brain, or procedures, where the actual signals in the brain are being monitored, for instance electroencephalography.

- *Å. Birkeland is with the Department of Informatics, University of Bergen, Bergen, Hordaland, Norway. E-mail: aasmund.birkeland@gmail.com.*
- *C. Turkay is with the Department of Computer Science, City University London, Room: A304C, Northampton Square, London EC1V OHB, United Kingdom. E-mail: Cagatay.Turkay.1@city.ac.uk.*
- *I. Viola's is with the Institute of Computer Graphics and Algorithms, Vienna University of Technology, Favoritenstrasse 9-11, E186, Vienna 1040, Austria. E-mail: viola@cg.tuwien.ac.at.*

Manuscript received 27 Jan. 2013; revised 24 Mar. 2014; accepted 10 Apr. 2014. Date of publication 6 May 2014; date of current version 1 Nov. 2014. Recommended for acceptance by D.A. Bowman.
For information on obtaining reprints of this article, please send e-mail to: reprints@ieee.org, and reference the Digital Object Identifier below.
Digital Object Identifier no. 10.1109/TVCG.2014.2322363

In psychophysics, investigation is performed by examining how physical stimuli can affect the perception in subjects. For motion detection, this is typically performed by providing a task to the user, based on a certain stimulus. Analysis is then based on examining correlations between the parameters in the stimulus and the response given by the user.

In this paper we have evaluated the perception of a speed-up factor of one motion pattern with respect to another motion pattern. We analyzed how the relative motion perception is affected by four distinct parameters: relative speed up factor between two sets of particles (speed multiplier), global scale of the velocities (the overall speed of particles moving across the screen), chromatic and luminance contrast, orientation, and direction of motion. In addition, we have tested for any influence by adding visual cues, in form of comet tails, and the point distribution (Poisson distribution versus random). We have performed user studies where we measured the subjects' estimation of relative speed between two separate sets of moving particles. We have discovered significant trends in estimation error for two of the parameters, speed multiplier and global scale of the velocities. The main contribution in this paper is the first compensation model for creating a perceptually uniform motion space, when using animated particles in visualization. From a series of perception studies we have shown how the compensation model successfully compensates for the effect of selected parameters. From our studies, we have shown how adding multiple visual cues, have a small improvement in perceived speed of animated particles. In addition, we provide statistical indication that the effect of chromatic versus luminance contrast are not as prominent on currently most widely used LCD monitors, as presented in previous work.

2 Related Work

In order to understand how the human visual system is detecting and analyzing motion, there are several aspects that come into play. For instance, a typical view on problems in vision is that they can all be modelled as correspondence problems. Finding the correspondence of an object compared to the brain's representation of that same object is used in object recognition. In motion detection, the problem can be modelled as detecting correspondence over time. As a computational problem, motion detection can be seen as detecting changes in a given position. The *Reichardt detector* [8] is an implementation based on finding the correspondence over time.

In contrast to the Reichardt detector, an alternative model for motion detection involves finding change in luminance over time, known as the *temporal derivative*. A more detailed explanation can be found in related literature [9].

From a psychophysics perspective, we find much work in experimentation on the effect of different parameters when users evaluate motion. Experiments suggest that contrast change has an effect on the perception of the given speed [10], [11]. However, there is controversy regarding how this affects the perceived speed in general [12], [13].

Research indicates an impact of color and luminance to motion detection. A continuous change in luminance can create apparent motion of stationary objects [14]. Derrington and Henning presented a study on the impact of color to the motion after-effect [15]. Backed up by the claim of color and motion being processed in parallel in the human visual system, evidence has indicated that applying only chromatic contrast compared to luminance contrast will cause a slow down in the perceived velocity [16], [17].

There exist rules which approach the subject of perception and how it scales to different stimulus. Weber's law is introducing the term *Just Noticeable Difference*, which means that the smallest difference between two stimuli is proportional to the absolute magnitude of the stimuli. Fechner's law states that the subjects' impression of a stimuli is proportional to the logarithm of intensity of the stimuli. In addition, there is Steven's power law [18], which is a more generalized description of the relationship between perception and stimulus. More details are found in existing literature [19], [20], [21], [22], [23].

Most work in motion detection results in qualitative statements that mainly explain the effect of a given stimulus. Little information is provided regarding how to compensate for any systematic distortions in the human visual system. In color theory, there exists a compensation model which creates a perceptually uniform color space called CIE 1976 (L*, a*, b*) color space (CIELAB). In the context of motion, a similar model would aid visualization techniques based on moving elements in conveying the correct information according to the underlying data. A similar approach in the domain of 3D shape perception is taken by Šolteszova et al. [24]. In this work, the authors modify 3D shapes by building a statistical model of the error in perceiving shapes. Although in a different domain, this paper also demonstrates how visual representations can benefit from considering the perceptual aspects of the viewers.

We can explain our goal for this paper by drawing an analogy to color theory. As CIELAB is a color model where the perceptual difference for each step in the color space is uniform, we intend to create a compensation model for moving particles, which can compensate for systematic distortions in the visual system when estimating relative motion. This way, we can apply animated particles in visualization in a manner where the perceived information correlates better with the underlying data.

3 Methodology

In order to create a compensation model for a given set of parameters, we need to find the impact that each parameter has on the perceived relative motion. For estimating relative motion of animated particles, there are several parameters which can affect how a subject estimates motion. The density of particles, the size of the particles, contrast level between particle and background, contrast type (luminance or chromatic), relative difference in speed between particles, direction of motion, global scale of the velocities, shape of the particles, all can affect velocity estimation in different ways.

For our compensation model, we first selected a sub-set of the possible parameters to investigate. To assess a proper range for the parameters and the performance of our test-design, we performed a pilot study with a small set of

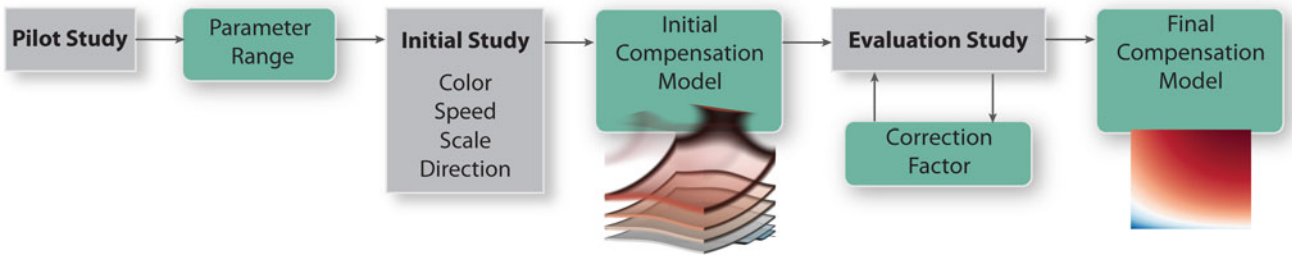

Fig. 1. Process pipeline for achieving perceptually uniform motion space. We started with a pilot study to determine suitable ranges in parameter space. From the pilot study, we designed an initial study to investigate the selected parameters. The output was an initial compensation model. In the evaluation stage, we performed two iterations to determine the efficiency of our model and adapted the model according to the new results.

participants. After adjusting the study based on observations from the pilot stage, we performed a larger study to find the trends for each selected parameter. Using the resulting trends we discovered in the initial study, we created an initial compensation model and started an iterative study process to test and refine the model. An illustration of the process is depicted in Fig. 1.

We started with a study using a simple setup, with basic particles with a uniform distribution and size. For a basic set of parameters, we chose four parameters that are seen frequently in visualization techniques using animated particles. Examples of tasks involving each parameter can be seen in Fig. 2.

First, there is the range of screen-space velocities for the particles. When looking out the window of a fast moving car, it is difficult to clearly see stationary objects, like trees or road signs, close to the car. Based on this effect, we can deduce that there is a speed limit in the visual sector, for which humans can perceive objects clearly. We assumed that speed estimation would be affected by this effect as velocities would approach the limit of the visual system. To investigate this, we chose a parameter which would scale

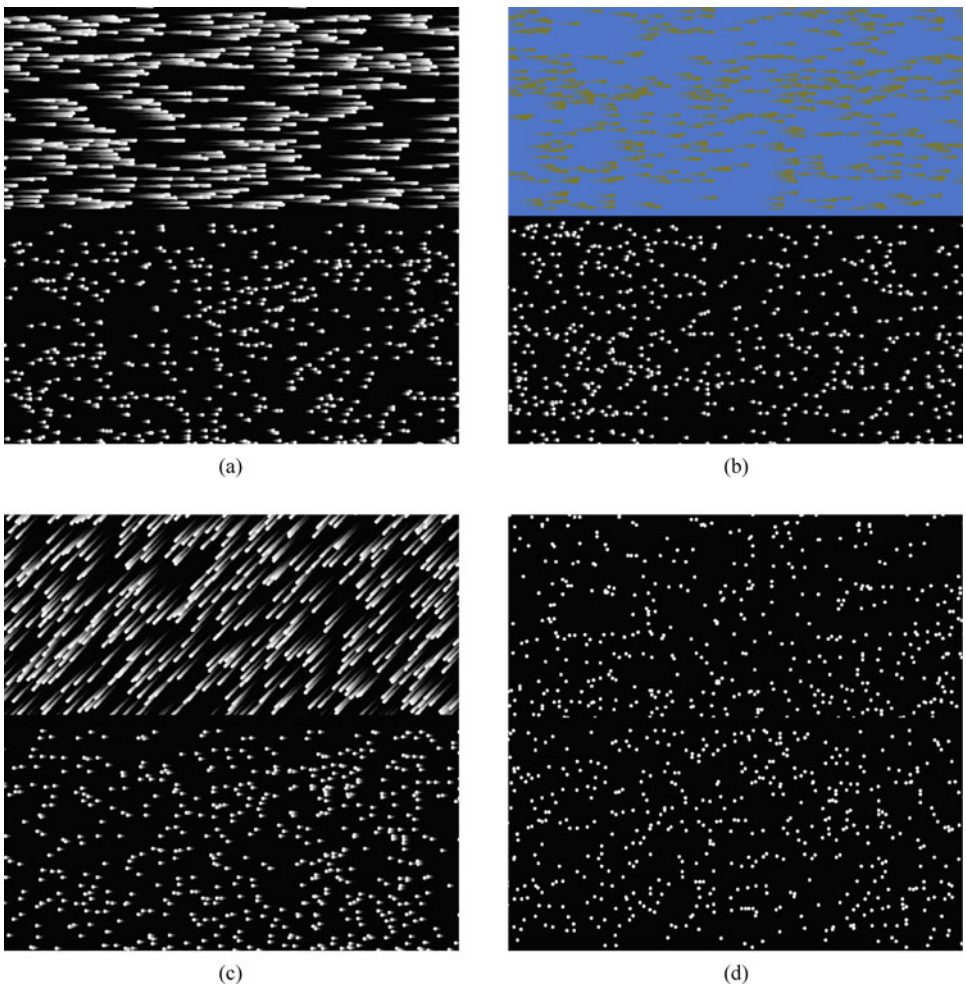

Fig. 2. Screenshots from tasks with different parameter settings. 2a shows a basic setup with direction angle set to 0 degree and the speed multiplier set to 5. 2b shows chroma only contrast. In 2c, the direction of the flow was set to 45 degree down and to the left. 2 d shows the basic particles without a tail.

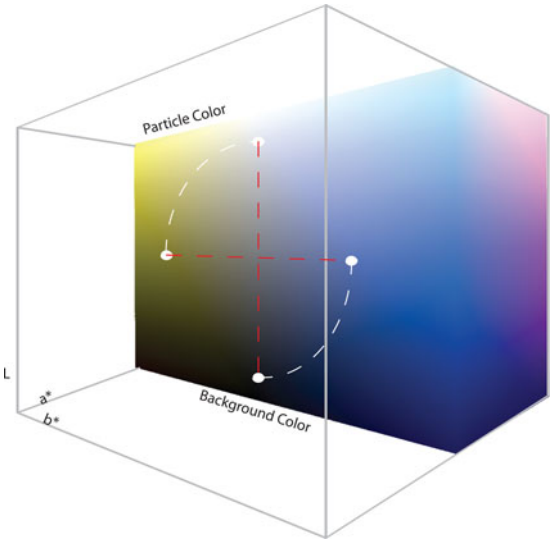

Fig. 3. The contrast-type parameter was set to be the angle of two points circling around a center point in CIELAB color space. 0 degree gave two colors with no chromatic contrast, and 90 degree returned two colors with only chromatic contrast, while always maintaining a constant contrast level.

up the speed of the animated particles globally, namely *global scale of velocities*.

Due to the asymmetries in horizontal and vertical vision [9] (e.g., due to the fact that our eyes are aligned horizontally), we draw the assumption that there would be a change in the perceived motion when viewing particles moving from left to right rather than moving from top to bottom. In addition, comparing motion when particles are moving in the same direction would be easier than comparing motion in the opposite direction. We chose to test for this effect by introducing a parameter which would set the direction of the particle motion. Direction ranged from 0 to 359 degree, where 0 degree meant the particles were moving in the same direction.

It has been stated that change in contrast and color can affect the perceived motion [17]. When mixing color coding and motion in visualization one should then be careful about the resulting contrast between the moving particles and the background. Based on the experiments presented in previous work, we assumed there would be a trend in estimation error as the contrast type would change from luminance-only to chroma-only. To adjust the contrast type, we generated colors by selecting points in CIELAB color space with luminance only. To shift the contrast type we rotated the points around the center-point within CIELAB color space up to 90 degree. 0 degree would then result in two colors with luminance-only contrast, and 90 degree would result in two colors with chroma-only contrast. The contrast level would remain the same for all degrees. Fig. 3 illustrates how the colors were selected.

As the difference in speed between the reference and test stimulus increases, we assumed that the perceived difference would not scale linearly. The main parameter tested was speed multiplier between two sets of moving particles. This corresponds to the theory of *Just Noticeable Difference*, meaning that the smallest difference we can detect, is connected to the intensity of the certain input. If the absolute speed of the particles is high, the absolute difference between them should be comparably high.

We investigated the effect of adding additional visual cues, which would indicate the speed of the particles. To test if additional visual cues improved the perceived speed, we added comet tails to particles for half of the tasks generated. The length of the comet tails were linearly scaled by the speed of the particles and had a linear drop-off in width and opacity. We also tested for any influence of the distribution of the points drawn on the screen. A short pilot study was performed where half of the tests used a Poisson distribution and the other half used random sampling.

While contrast type and direction has a natural limit of range, the range of global scale and speed multiplier has no such limit. However, it is natural to assume that there is a certain limit for these parameters, where the error in estimation becomes too large to be clearly connected to the underlying data. In the pilot study, we found that estimating speed for particles moving with a velocity over $41.5\ \mathrm{degree/second}$ in the visual sector, the deviation in error becomes so large that any estimation from a user becomes meaningless when linked to the data. In addition, if the velocity magnitude of one set of particles became more than six times the velocity magnitude of another, the error in estimated speed multiplier became too high to be useful. We set the base speed to $0.83\ \mathrm{degree/second}$, which constitutes one pixel per frame at 30 frames per second. This prevents any jitter in the movement of the particle. With a base level of $0.83\ \mathrm{degree/second}$, the range of the global scale parameter was set to 1.0 to 7.0. With a maximum speed of $41.5\ \mathrm{degree/second}$, we set the range of the speed multiplier to range between 1.0 to 6.0.

4 Test Design

The aim for the study was to test for perception of relative speed between particle sets. In particle based visualizations, there is a multitude of variations in complexity among particle types, size, density, direction of motion, flow topology and more. To investigate the perception of relative motion, we made a deliberate decision to start with a basic setup, which would test only one parameter at a time. This way, we can remove any unforeseen effects from other parameters.

In our tests we have two sets of particles displayed on the screen. One set is displayed at the top half of the screen (*test particles*) moving at a velocity $\mathbf{v}_t$, and one set is displayed at the bottom half (*reference particles*) moving at a velocity $\mathbf{v}_r$. The user was then asked to provide the multiplication factor, s, which satisfies the equation:

$$|\mathbf{v}_r| \cdot s = |\mathbf{v}_t|. \tag{1}$$

We have chosen to design the stimulus as a juxtaposition of two stimuli [25]. An alternative would be a superposition of the two stimuli, but this design will suffer from particle mixture and mutual occlusion. In such a case additional cognitive load will be required to isolate these two stimuli from each other, prior to the comparison.

The juxtaposition design has one problem though. When the two stimuli are far away from each other, the subject has

to frequently move the eyes to switch the focus. Therefore, in our study we have placed the stimuli as close to each other as possible. This allows the foveal and parafoveal vision to take part on the visual processing, without the need of frequent refocusing from one stimulus to another one.

Change in density as well as a repeating pattern can distort the perception of speed. To compensate for this, the particles for each half were generated randomly under the constraint that the average spatial distribution remained uniform regardless of velocity and direction similar to the experiments performed by Geesaman and Qian [26] or Watamaniuk et al. [27].

However, the random generation of particles might lead to structures in the motion pattern, i.e., several particles clustered together due to randomness in the distribution. To investigate whether such structures affect the test results, we perform an initial pilot study that compares our randomly distributed particles with those that are regularly distributed. In order to create moving particles that are regularly distributed, we generate our particles following a Poisson Disk distribution as suggested by McCool and Fiume [28]. We performed a small test with three subjects, where each subject completed 100 tasks. We then check whether there is any significant difference when particles are regularly distributed, we observed that the estimation error with the regularly distributed particles was slightly higher, i.e., average error -0.0416 with random versus -0.0991 with regular points. However, this difference was found to be insignificant with a p-value of 0.3412 when a regular two sample t-test was applied. Due to this result and due to the slightly better performance in error, we continue our study with randomly generated particles.

We selected subjects from various ages, gender, and professions. Each user was given a set of 100 tasks. To avoid any learning curve, we excluded previous participants for the consecutive experiments. The subjects were not informed of the parameter intervals and were told to estimate velocities based on visual impression and not from explicitly timing particles' traversal over the screen (for example by counting seconds and comparing distances). For the four rounds of user studies, we invited 10 participants for the pilot study, 22 for the initial round, 10 for each of the evaluation rounds.

For every test subject we used a 24-inch screen with a 16:10 aspect ratio. The pixel size was 0.27 mm and the canvas dimension was set to 768×768. The user's head was approximately 50 cm away from the screen. While traditional CRT screens are typically used for experiments, we used modern LCD screens, which have sufficient quality for our experiments [29] and, more importantly, are utilized nowadays, in contrast to the CRT monitors that are practically not in daily use any longer. Wang and Nikolic stated that the use of LCD can in some cases be preferred, but not when the image changes rapidly. For our case, the smooth motion makes it beneficial to use LCD. In addition, the changes are not rapid. A small blur will appear from the points, but similar to the comet tails, this has a very little effect to the perceived stimulus as are shown in the results in Table 3. Another challenge with LCD screens is representation of color. While the LCD screens might not provide an absolute iso-luminant contrast, our motivation is driven by real world application, and in a real world scenario, optimal conditions are never fully achieved. In most real world situations, the user will use an LCD screen with default settings.

If the eye is fixated on a continuous motion over some time, the eye will *adapt* to the motion. The reason for this is an effect called neural adaptation [30], where the neurons coding the particular motion reduce their responses. This can result in a distortion of our test. To avoid direction fatigue for the base speed, we alternate the direction of the flow for every other test. Furthermore, the subjects were asked to take a two-minute break after each 25 tasks have been completed.

The test design remained unchanged for the three iterations of testing.

5 User Studies

5.1 Creating the Compensation Model

In the first round we wanted to investigate the effect of the selected parameters separately. We generated three types of tasks, one which tested the effect of global scaling of the velocities. The scaling is added on both sets of the particles. This changes Equation (1) to:

$$|\mathbf{v}_r| \cdot s \cdot \sigma = |\mathbf{v}_t| \cdot \sigma. \tag{2}$$

The range of σ was 1.0 to 7.0 and the range of s was 1.0 to 6.0. For all the tasks involving global scale, the color-parameter remained constant at 0 degree and the motion direction remained strictly horizontal.

The second type was aimed for contrast type. We generated tests where colors were selected with the scheme explained in Fig. 3. The parameter ranges of 0 to 90 degree in CIELAB color space. The range of s was 1.0 to 6.0. The global scale parameter σ was constant at 1.0 and direction remained strictly horizontal.

Finally we tested for the direction of the flow in the range of 0 to 359 degree direction. For each task we queried the subjects for speed multiplier between the two sets of particles in the range from 1.0 to 6.0. The global scale parameter σ was set to 1.0 and color-parameter was set to 0 degree.

For each parameter tested, we created tests with random configurations within the given parameter space. For instance for contrast-type, a configuration might be as follows: $\sigma = 1$, $s = 2.3$, color-parameter $= 90$ degree and direction $= 0$ degree. To prevent samples from being too clustered in the parameter space, we constrained a random function to keep the same number of tests within each interval. In total 2,220 tasks were generated for the initial study. When the study was completed, outliers were removed. We utilized a visual inspection of the results supported by the Mahalanobis scores computed for each sample. Here we take a purely data-driven outlier-removal strategy, rather than considering specific participating individuals or the contextual properties of the test. In this stage, we compute a Mahalanobis score for each sample using the speed multiplier versus signed estimation error. The threshold for outlier removal was 14.2, determined by visual inspection of the scores. This resulted in the removal of 22 outliers. The final sample size was then 2,198.

TABLE 1
Results of the General ANOVA Test Treating Each of the 10 Bins as a Separate Group

Parameter	F-value	p-value
Global Scale	9.9745	1.440×10^{-13}
Direction	0.7131	0.490
Speed Multiplier	8.6012	9.176×10^{-13}
Chroma vs. Luminance	0.8376	0.5816

The high p-value show that there are no significant trend in estimation error compared to direction and contrast type.

From the results of the initial study we examined the relation between signed error and the parameters, i.e., if test-subjects overestimate or underestimate the *speed*. The trend in signed error is more relevant than unsigned. As there is a general trend in overestimation, we can compensate for this by slowing down the test particles. By this we will achieve a closer match between human perception of relative speed and the intended information communicated via the visualization.

We investigated the estimation trend for each parameter. The significance of the trends was evaluated by binning samples in parameter intervals. To provide a more robust significance evaluation, we performed statistical tests for different parameter intervals. In the following, we discuss the tests with 10 bins for each parameter. We start by applying a one-way Analysis of Variance (ANOVA) test by treating each bin as a separate group. When we observe the results for this general multiple group test, we see that there is a significant difference between the groups for the global scale and the speed multiplier parameter. However, for the direction and chroma parameters, we observe no overall significant difference between the multiple groups (refer to Table 1 for the corresponding results). In order to achieve more detailed results to explain the trends within the parameter intervals, we perform post-hoc tests. We prefer to do a *two-sample unpooled t-test with unequal variances* between each bin and the bin at the initial parameter setting. We follow this strategy (i.e., initial bin versus the others) since the parameter intervals are ordered and we want to investigate the trends in relation to this ordering. Moreover, we observe that the variance of the data is not equal within different intervals so we assumed unequal variances in our tests. Table 2 displays the t-scores for each parameter. The table shows the results from having 10 bins for each parameter. Interval shows the bin size in parameter space. N is the number of samples in the bin. Mean shows the average in signed estimation error and T-score shows how the bin compares to the top row. DoF indicates the degrees of freedom for the t-test. Since the different intervals contain samples from the same individuals under different conditions, i.e., varying parameters, we calculate the degrees of freedom accordingly and use $n/2 - 1$ as the formula where n is the total number of observations in the both groups. One point to mention here is that we checked for normality (using a Shapiro-Wilk Normality Test) on each of the bins prior to performing the tests whether to use non-parametric tests instead. We observed that for some of the bins, the

TABLE 2
Results from the *Two-Sample Unpooled T-Test with Unequal Variances*

Direction				
Interval	N	Mean	T-score	DoF
0 - 36	150	-0.126	0.000	149
36 - 72	141	-0.155	0.682	145
72 - 108	142	-0.110	0.352	146
108 - 144	148	-0.094	0.722	148
144 - 180	145	-0.158	0.729	148
180 - 216	149	-0.220	2.054	148
216 - 252	146	-0.170	1.058	147
252 - 288	145	-0.107	0.424	148
288 - 324	128	-0.106	0.440	138
324 - 360	144	-0.155	0.745	146
Global Velocity Scale				
Interval	N	Mean	T-score	DoF
1.0 - 1.6	40	-0.206	0.000	39
1.6 - 2.2	34	-0.007	3.903	36
2.2 - 2.8	35	0.244	5.834	36
2.8 - 3.4	31	0.304	6.435	34
3.4 - 4.0	37	0.375	6.023	37
4.0 - 4.6	33	0.313	6.369	35
4.6 - 5.2	32	0.425	5.468	35
5.2 - 5.8	36	0.594	7.804	37
5.8 - 6.4	28	0.530	8.643	33
6.4 - 7.0	35	0.617	8.644	36
Speed Multiplier				
Interval	N	Mean	T-score	DoF
1.0 - 1.5	224	0.032	0.000	223
1.5 - 2.0	213	0.009	0.676	217
2.0 - 2.5	217	0.011	0.571	219
2.5 - 3.0	221	-0.016	1.279	221
3.0 - 3.5	216	-0.015	1.172	219
3.5 - 4.0	228	-0.099	3.464	225
4.0 - 4.5	187	-0.135	5.158	204
4.5 - 5.0	263	-0.112	4.165	242
5.0 - 5.5	207	-0.153	5.400	214
5.5 - 6.0	222	-0.200	7.144	222
Chroma vs. Luminance				
Interval	N	Mean	T-score	DoF
0 - 9	35	-0.104	0.000	34
9 - 18	47	-0.127	0.344	40
18 - 27	48	-0.133	0.405	40
27 - 36	40	-0.154	0.772	36
36 - 45	39	-0.176	1.164	36
45 - 54	39	-0.052	0.712	36
54 - 63	42	-0.102	0.032	37
63 - 72	38	-0.059	0.572	35
72 - 81	50	-0.145	0.681	41
81 - 90	41	-0.156	0.739	38

A significant correlation can be seen for the speed multiplier and global velocity scale parameters. For the direction parameter only a weak correlation can be seen, at around 180 degree. Unlike previous work, we could not detect any significant trend from change in contrast type. Here the results are collected into 10 bins for each parameter. Interval column indicates the parameter range for each bin. N is the number of samples in each bin. Mean shows the average in signed estimation error and T-score shows how the bin compares to the top row. DoF indicates the degrees of freedom for the t-test, where it is calculated as $n/2 - 1$ (n being the total number of samples) to account for repeated measurements.

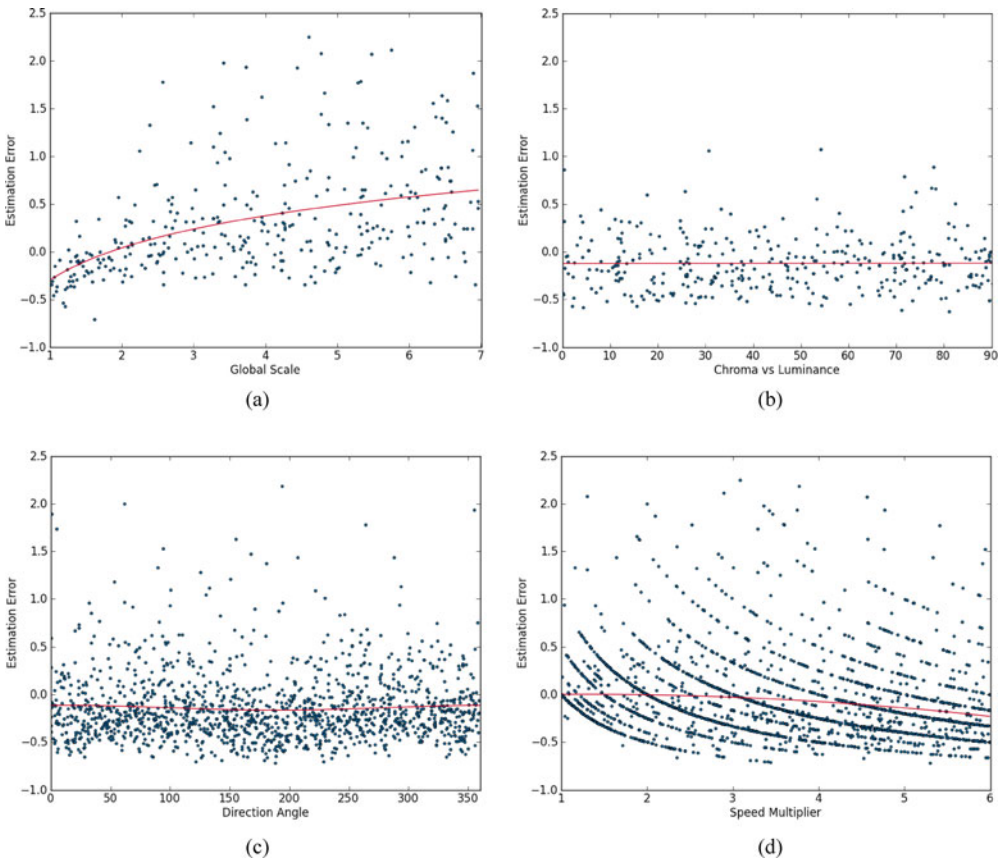

Fig. 4. Scatter plots of the samples generated from the first perceptual study round. The red curve shows the regression curves used for the compensation model. The curve for chroma-type (4b) shows no specific trend and thus this parameter was not included in the compensation model.

normality condition was not met. However, we still prefer the parametric t-tests since they provide us an insight on how the error evolves over the consecutive intervals.

We assumed that there would be a trend in estimation error which correlated with the relative motion between the two sets of particles. From Table 2, we can see there is a trend to continuously underestimate the speed value as the speed multiplier is increasing. Fig. 4d shows a scatter plot of the error in estimation compared to the speed multiplier parameter.

The results from the initial study also justify the assumption that there would be a change in estimation as the global scale of the velocities increases. Unlike the speed multiplier, subjects move from an underestimation to an overestimation. However, the slope for the regression curve for the relative motion factor remained unaffected by the global scale parameter.

We had a hypothesis that comparing particles moving in different directions would be more difficult than comparing particles moving in parallel to each other. The difference in direction, however, seems to have a very small impact on the estimation error. From the results we could only find a significant correlation in unsigned error. There was, however, a weak correlation in the signed estimation error. This leads to the conclusion that direction should be accounted for in our compensation model.

Based on previous experiments in prior work [17], we expected to see a general trend in underestimation when using iso-luminant contrast. However, we were unable to detect any *slow-down* effect in our experiment. Fig. 4b shows the impact on the estimation error related to the contrast-type.

In addition, Table 3 shows the measured effect of the added visual cue. The effect is small and only prominent for animated particles with higher velocities.

The overall goal was to detect which parameters caused a trend in estimation error, which in turn, could be compensated for in particle-based visualization. From analyzing the result, we found strong correlations between speed multiplier and scale when comparing them with the estimation error. We also found a weak correlation between direction and estimation error. Therefore we chose to include the three parameters into our compensation model. We also checked for dependence between these parameters using

TABLE 3
This Table Shows the Mean Error and Standard Deviation of the Estimation Error for Each Task Type, Compared to the Overall

Parameter	Tail	Mean Error/Std. Dev.
All	without	0.335 / 0.283
	with	0.299 / 0.271
Global scale	without	0.489 / 0.489
	with	0.375 / 0.432
Contrast type	without	0.253 / 0.182
	with	0.250 / 0.174
Direction	without	0.321 / 0.219
	with	0.296 / 0.240

Comparing the tasks where the additional perception cue was taken into account, there is a 3.6 percent decrease in mean error and standard deviation goes down by 1.2 percent.

TABLE 4
Regression Line Parameters Fitted to Test Results

Constant	Value
a_s	-0.010414
b_s	0.02680727
a_d	0.0261351
b_d	-0.16202086
c_d	-0.14056624
a_σ	0.48538867
b_σ	0.29785412

Pearson's correlation test and observed no significant dependence within any of the parameters.

To create the compensation model we needed a function to describe the trends in the estimation error. For the global scale, we choose a logarithmic function,

$$E_\sigma(\sigma) = a_\sigma \cdot \log(\sigma) + b_\sigma, \tag{3}$$

where σ is the global scale and a and b are constants defined in Table 4. The logarithmic function gave a slightly worse fit compared to a second order polynomial, but since the first order derivative became negative at 6.5 in parameter space, we found the second order unsuitable to describe the trend, since the average estimation error was not decreasing (see Table 2).

To find a function for the effect of direction, we fitted a periodic cosine function,

$$E_d(\alpha) = a_d \cdot \cos(\alpha + b_d) + c_d, \tag{4}$$

where α is the angular difference between the two sets of particles and a, b and c are defined in Table 4. Since the trend in error is cyclic, we found the cosine function to be better suited than a higher order polynomial.

Finally, we fitted a second order polynomial function for the speed multiplier parameter, which we constrained to be zero when the particles were moving with the same speed,

$$E_s(s) = a_s \cdot s^2 + b_s \cdot s - (a_s + b_s), \tag{5}$$

where s is the speed multiplier, and a and b can be looked up in Table 4.

Each function provides an estimated error for the given parameter. The final compensation function should provide a scaling function for the velocity to compensate for the total error from all parameters. In addition, the average error at the base level for each parameter would be contained in each function. This was solved by only including the change in error for the scale parameter and the direction parameter. The compensation function combines the error functions in the following manner:

$$\begin{aligned} C_\sigma(\sigma) &= 1 + E_\sigma(\sigma) + E_\sigma(1) \\ C_d(\alpha) &= 1 + E_d(\alpha) + E_d(0) \\ C_s(s) &= 1 + E_s(s) \\ F_c(\sigma, s, \alpha) &= \frac{1}{C_\sigma \cdot C_d \cdot C_s}, \end{aligned} \tag{6}$$

where F_c is the final compensation function, graphically depicted in Fig. 5.

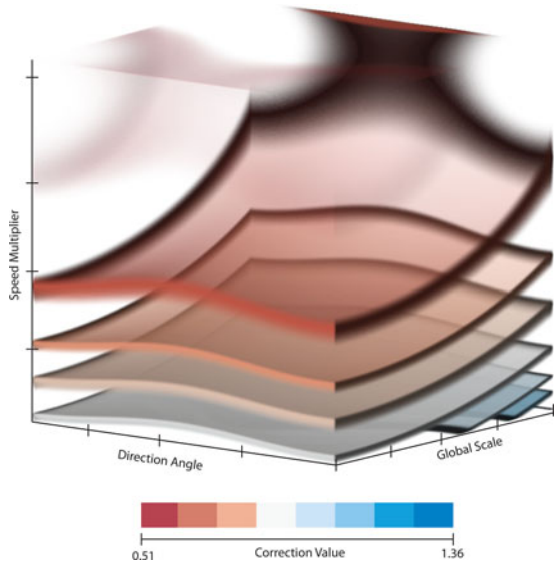

Fig. 5. A volume rendering for the 3D function defining our compensation model.

Before we move on the two following sections where we present our evaluation and adjustment of the compensation function, we first present how our model can be evaluated in relation to the psychophysics literature, in particular to Steven's power law [18].

5.2 Validation against Psychophysics Theories

In our method described above, we take a linear approach in computing the errors between the reference and test displays, and we compute the difference between the multiplication factor we set and the one given by the user. Here, we validate this error computation approach with a comparison to Steven's Power Law theory [18] from psychophysics literature.

As briefly mentioned in Section 2, Steven's theory states that there is a non-linear relationship between perception and stimulus that follows a power law function in the form $y = kx^a$. If we apply this to our case where the stimulus is the velocity of the *test particles* $\mathbf{v}_t$, this formula turns into $\mathbf{v}_{pr} = k\mathbf{v}_t^\lambda$. Here, $\mathbf{v}_{pr}$ indicates the velocity (of particles) that subjects should be perceiving according to Steven's theory.

Following Steven's theory, we adjust the ground truth while evaluating the s values that subjects provide for each test. This leads to new error values and distributions. Refer to Appendix for further details on how these computations are carried out. We first compute the mean of the error distributions for the new values. The average error for the global scale related tasks is 0.290 when the modified error values are considered. When compared to the previous error distribution, we observe no significant difference. However, for the other tasks (i.e., chroma versus luminance and direction), the average error values are significantly lower, indicating an overall underestimation. This is very likely due to the fact that in these other tasks speed difference is not the only varying stimuli and a more complex psychophysical is needed.

We now focus our attention to check whether we observe similar trends in estimation error when the error values are

TABLE 5
Results of a General ANOVA Test Treating Each of the 10 Bins as a Separate Group with Errors Computed by Considering Steven's Power Law

Parameter	F-value	p-value
Global Scale	3.9193	9.4186×10^{-5}
Direction	0.4316	0.6494
Speed Multiplier	74.9567	4.9585×10^{-121}
Chroma	0.5580	0.8312

computed according to the Power Law model. In order to do that, we perform a one-way ANOVA test following the same procedure used earlier in this section, i.e, the process that led to Table 1. When the new error distributions are used in the ANOVA test, we arrive at the same result with our approach—there is a significant difference within the bins only for the global scale and speed multiplier parameters (see Table 5). This shows that our earlier observations are in line with the power-law-modified computations.

Moreover, we use the new error distributions to fit the same functions we use earlier in this section to perform a further comparison. We compare the *coefficient of determination* scores [31] (i.e., R^2) for both our functions and the new functions fitted to modified error values. We observe that our functions fit better to the data compared to power law functions.

These reported observations demonstrate that our compensation model is in agreement with the previous related studies that fit Steven's Power Law functions to human psychophysical data and thus provides additional support for the validity of our model.

5.3 First Evaluation Study

After we built the initial version of the compensation model, we continued the process by evaluating it through a new round of perceptual study. Our aim at this stage was to assess the changes in the results due to the modifications by the compensation model. We then aimed to improve the model further, as a result of the investigation of the results from the new user study.

In this second round of the study, we made tests to evaluate the three parameters, namely, speed multiplier, direction of motion, and velocity scale. Note that, we left out the contrast parameter at this stage. We randomly created 486 different combinations of these parameters to build the tasks for this round. For each of these parameter combinations, we created two separate types of tasks. In the first task, the final velocity was modified by the compensation model (i.e., experimental group), and, in the second task the final velocity was set without any modification (i.e., control group). This process led to $486 \times 2 = 972$ tasks in total. Similar to the previous round, we used particles with tails for half of the 486 parameter combinations. The tasks were then distributed randomly to 10 subjects, who have not taken part in the first part of the test.

We started analyzing the results by performing an outlier analysis of the results. First, we removed the corresponding tasks from two specific users since their results exhibit conflicting trends when compared to both the 22 users in the first round and the other eight users in the second round. Additionally, we removed 16 results after an inspection of their Mahalanobis scores. Here, we use two Mahalanobis scores computed using two sets of variables, 1) speed multiplier versus estimation error 2) global scale versus estimation error. The threshold to mark samples as outliers are 8.3 for the first score and 7.8 for the second. After the outlier removal, the remaining set consists of 756 task results.

To evaluate the impact of our compensation model, we treat the experimental and the control group separately (with/without modification). We observe the effect of each parameter on the estimation error separately. In order to do that, we plot the estimation error against the three different parameters for both of the experimental and control group. These plots can be seen in Fig. 6. Moreover, we fitted regression lines to each plot (Table 6) and computed the average estimation error for the two groups of tasks.

For the tasks that are modified with our compensation model, both regression lines highlight a very significant result. We observe that our compensation model manages to flatten out the estimation error trends for both parameters. Specifically, for relative motion the estimation error trend slope goes down from -0.05 to -0.005, and for velocity scale the slope goes down from 0.07 to 0.005. This amounts to an approximately $90\text{-}93\,\text{percent}$ improvement for the trends in estimation error.

Although the correlation between these parameters and the error is removed, the results show that our modifications lead to an overall underestimation of the velocities. This is clearly seen when the average signed estimation error is observed. The average signed error changed from -0.06 to -0.26. The same observation is also supported by the placement of the regression lines in the second column of Fig. 6, i.e., the regression line is below the x-axis. This

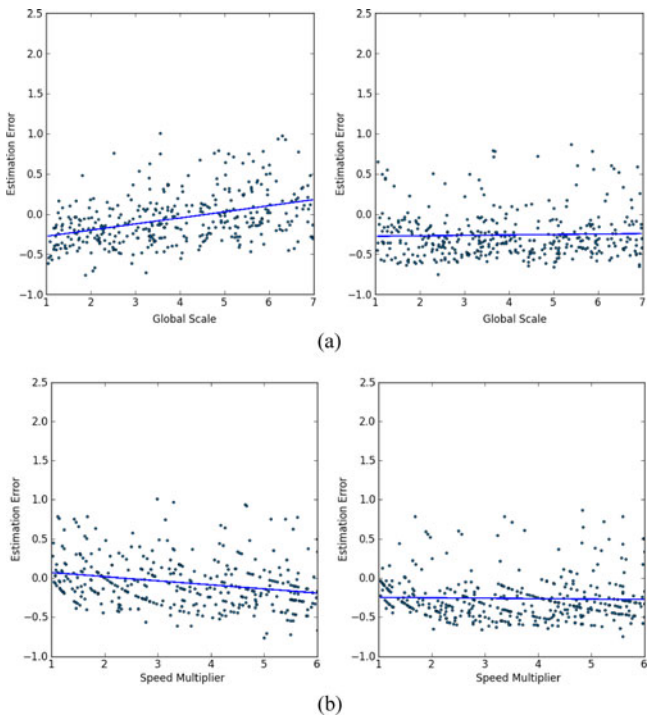

Fig. 6. The regression curves from samples generated in the first evaluation round. The different curves show without (left) and with (right) our compensation model.

TABLE 6
Regression Line Parameters Fitted to Test Results with/without Modification

Parameter	Modification	Slope	Intercept
Speed multiplier	without	-0.05	0.120
	with	-0.005	-0.241
Global scale	without	0.076	-0.354
	with	0.005	-0.283

TABLE 7
Regression Line Parameters Fitted to Test Results with/without Modification

Parameter	Modification	Slope	Intercept
Speed multiplier	without	-0.051	-0.068
	with	0.007	-0.153
Global scale	without	0.064	-0.37
	with	0.015	-0.240

observation leads to a modification of the compensation model. We corrected the overall underestimation by inserting a constant ϵ into Equation (6), where ϵ is equal to the average signed error, i.e., -0.26.

A second modification to our compensation model relates to the *direction* parameter. In order to check for the correlation between estimation error (both signed and unsigned) and the direction of motion parameter, we first group the task results into 10 bins that correspond to 10 consecutive intervals of the motion direction parameter, i.e., each interval spans $360/10 = 36$. Second, we calculate the correlation between the signed/unsigned error and the direction of motion parameter over these 10 intervals. However, there is no significant correlation in any of these intervals. Therefore, we have left out the direction of motion parameter from our compensation model.

As a result of these two modifications, updated compensation model is formulated with:

$$\begin{aligned} C_\sigma(\sigma) &= 1 + E_\sigma(\sigma) + E_\sigma(1) \\ C_\epsilon &= 1 + \epsilon \\ C_s(s) &= 1 + E_s(s) \\ F_c(\sigma, s) &= \frac{1}{C_\sigma \cdot C_d \cdot C_\epsilon}. \end{aligned} \tag{7}$$

These modifications to the compensation model called for a second evaluation round to assess the efficiency of the updated model.

5.4 Final Evaluation Study

In the final round, we wanted to investigate whether the correction based on the constant found in the previous round would have the desired effect. In addition, we removed the compensation for direction as this parameter had no significant impact. The setup for the final study was almost identical to the previous study with 972 tasks, two sets with equal parameters leaving 486 with compensation from Equation (7), and 486 without any compensation. The tasks where generated using the same constraints from the previous study. Again, we performed the study with ten *new* participants.

From the results we again removed outliers using the Mahalanobis score. We computed the distance for global scale compared to estimation error, and relative motion compared to the estimation error. The distance threshold was determined by visual inspection resulting in threshold of six for the global scale parameter and ten for the relative motion parameter. In addition, samples from one user was deemed unusable, due to having trends conflicting with the other 39 subjects included from all the results. In total 81 samples were removed, leaving 892 samples for analysis.

The results from the final study are shown in Table 7. The average estimation error for sample without compensation was $-11.5\,\text{percent}$. For samples with compensation the average estimation error was $-17.8\,\text{percent}$. From the previous round we had an average estimation error of $-26\,\text{percent}$. Thus leaving the final improvement to be $8.2\,\text{percent}$ higher than the previous round.

The parameter impact showed similar improvement in the last round, as we can see in Table 7. In Fig. 8, we can see the regression curves for the tested parameters. The improvement in slope is most prominent for the speed multiplier parameter, the slope for global scale parameter changed from 0.064 to 0.015. We then conclude that the effect of both parameters have successfully been reduced by more than $75\,\text{percent}$.

Based on the results from the last study, we present the final compensation model as follows:

$$\begin{aligned} E_\sigma(\sigma) &= a_\sigma \cdot \log(\sigma) + b_\sigma \\ E_s(s) &= a_s s^2 + bs - (a_s + b_s) \\ C_\sigma(\sigma) &= 1 + E_\sigma(\sigma) + E_\sigma(1) \\ C_\epsilon &= 1 + \epsilon \\ C_s(s) &= 1 + E_s(s) \\ F_c(\sigma, s) &= \frac{1}{C_\sigma \cdot C_d \cdot C_\epsilon}. \end{aligned} \tag{8}$$

Where the constants can be found in Table 8. The function is shown as a color map in Fig. 7.

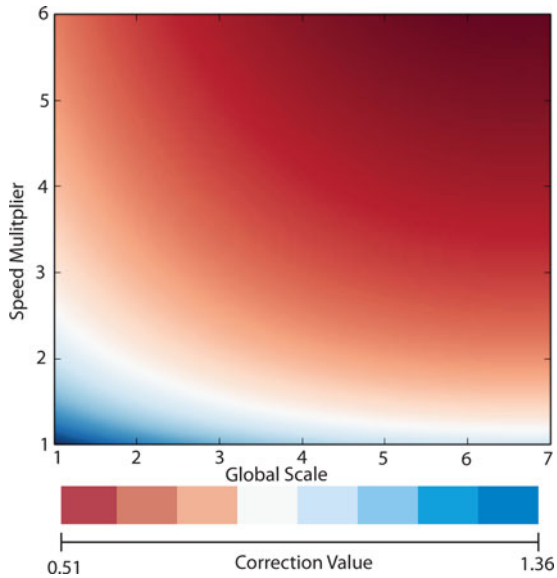

Fig. 7. The final compensation model resulted in a 2D function, depicted here as a height map.

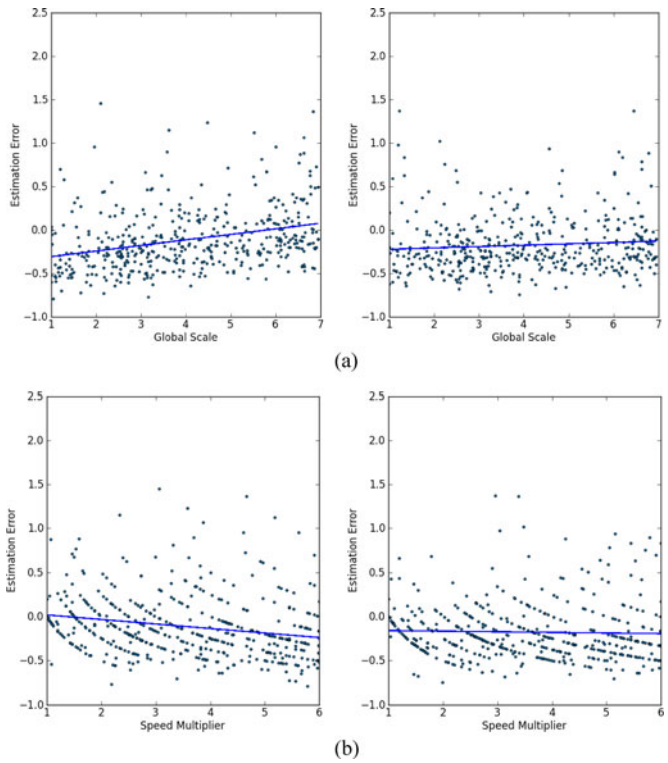

Fig. 8. The results from the final evaluation round. The different curves show without (left) and with (right) the adjusted compensation model.

6 Discussion

Experiments have shown that there was only a systematic change in estimation error when comparing two of the four parameters selected for our study, the speed multiplier and the global scale of the velocities. Increasing the speed multiplier, i.e., when the difference in speed was increased, the perceived difference seemed to scale at a lower rate. Also, when increasing the global scale of the velocities, the estimation error changed from underestimation at low speed (base-speed lower than approximately $1.66°/s$), to overestimation at higher speeds (above $1.66°/s$). In this case there seems to be a *sweet spot* where we are most likely to achieve the best estimation, without any compensation. The trend in estimation error compared to speed multiplier remained approximately the same throughout the range of the global scale parameter and should be accounted for.

Although, there was no systematic trend in the signed estimation error, when comparing to the direction of the flow, there was a change in the error magnitude. When

TABLE 8
Constants for Equation (8)

Constant	Value
a_s	-0.010414
b_s	0.02680727
a_σ	0.48538867
b_σ	0.29785412
ϵ	-0.26

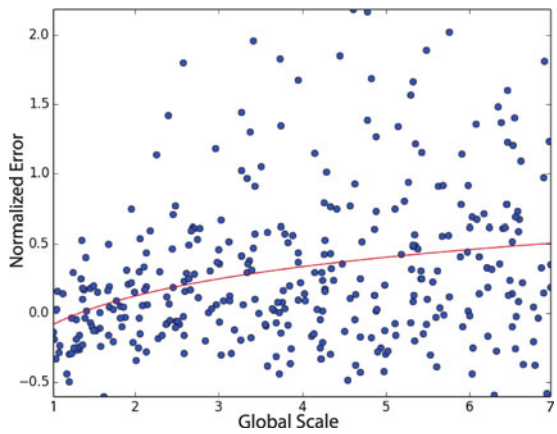

Fig. 9. Error distribution computed following Steven's power law versus the global scale test parameter.

the difference in direction approached $180\,\mathrm{degree}$, there was a small increase in error. However, due to the lack of any systematic change, we were unable to correct for this effect.

From the experiments in previous work, it has been reported a slow-down effect has been reported when gradually changing from luminance contrast to chromatic contrast. In our experiments, this effect was not reproduced. While we should be careful to rule out any impact from contrast-type completely, we might see that this slow down effect is caused not only by different types of contrast, but the gradual change. Mather [14] reported that a change in luminance can create an apparent movement of stationary objects, and it could be that this effect is affecting the perceived motion of moving objects.

From the results using multiple visual cues for velocity encoding, such as comet tails for example, we can only see a slight improvement from simple moving particles. The lack of improvement could indicate that the claim of using multiple visual cues improves the subjects' understanding of speed, is not as prominent as previously believed. However, for higher speeds, comparing tests with a higher global scale of velocities to the general average, there is an improvement of 11.4 percent in estimation error, shown in Table 3. In addition, our results only relate to perceived speed and not to direction, and the additional visual cue provides information not only about the speed, but also about the history of motion as well as that of the particle's current direction. In addition, the usage of comet tails enables the encoding of velocities in still images, which simple particles do not offer, as can be seen in Fig. 2.

To utilize the compensation model in a real world environment, there are certain aspects which should be considered. Since this scales the velocities of particles based on the underlying data, integrating the particle velocities in order to calculate its position becomes an issue. The reason for this is that the actual motion of a particle in the given flow would move at the velocity given by the flow, and arrival time and position would be distorted by the scaling from the compensation model. This can be resolved by scaling the reference frame. Still, the distortion might lead to a less comprehensible visualization. A more proper usage would be to integrate particles for a short time, in order to encode speed at certain position. For longer temporal integration,

other visualization techniques, such as stream lines, would be advised. It is also important to note that visual speed estimation of animated objects will not be very highly accurate. Using moving particles should be used more as an overview, and using a compensated model for depicting the velocities would create a better impression of what exists in the underlying data.

7 Summary and Conclusion

In this paper we have presented a new perceptually based compensation model for using animated particles in visualization. The compensation model is based on the results from a series of perceptual studies, investigating the perceived speed of moving particles. The main goal has been to assess trends in estimation error based on selected parameters. We chose to test for four different parameters, namely global scaling of the particle velocity, the velocity direction, contrast type (iso-luminant versus achromatic), and speed multiplier. Four rounds of studies were performed: A pilot study, an initial study, which was aimed for testing each parameter separately. A second study, which tested the performance of the compensation model. Finally, the last study was conducted to assess the improvements from the previous round.

The results showed that significant trends were only visible in two parameters, global scaling and speed multiplier. A weak trend was found in the direction parameter. Using the trends in estimation error, we constructed a model which can compensate and reduce the effect of each parameter. The improvement was confirmed with a new study where the different parameters were combined. The results from the second study showed a large improvement in the impact factor from the selected parameters. However, the direction parameter was deemed insignificant. In addition, we also found a constant underestimation in speed estimation. Finally, we adjusted our compensation model according to the underestimation constant and performed an evaluation study of the corrected model. This again confirmed the reduction in impact from the significant parameters, as well as it improved the error in estimation compared to the previous study. This work was aimed at 2D flow, and can be used as a starting point for the perception of moving particles in 3D.

The final output from this work is a compensation model for the perceived speed of moving particles. Based on the global scale of the velocities and their relative speed-up factor, we have made an initial step towards a perceptually uniform motion space for animated particles.

Appendix

Applying Steven's Power Law

As discussed in Section 5.2, we support the validity of our approach by modifying the error computations in line with Steven's Power Law [18]. Here, we give details on how we represent the error in velocity estimations in our tests.

Assuming that the human perception of velocity follows a Power Law model, the test subjects perceive the reference speed $\mathbf{v}_r$ according to the following function:

$$\mathbf{v}_{pr} = k \cdot \mathbf{v}_r^{\lambda}, \tag{9}$$

where $\mathbf{v}_{pr}$ is the perceived velocity. Subjects responded with a estimated speed multiplier between the reference speed and the test speed (i.e., trying to estimate s in Equation (1)). So, the above formula becomes:

$$\mathbf{v}_{pr} \cdot s_s = k \cdot (\mathbf{v}_r \cdot s)^{\lambda}, \tag{10}$$

where s_s is the multiplier given by the subject as a response to the test, and s is the true speed multiplier. Since, $\mathbf{v}_{pr}$ is not known in Equation (10), we replace it with Equation (9) to get:

$$(k \cdot \mathbf{v}_r^{\lambda}) \cdot s_s = k \cdot (\mathbf{v}_r \cdot s)^{\lambda}. \tag{11}$$

We solve this Power Law model by linearizing this function through taking the log of both sides and estimate the k and λ values, in our study these values are found to be $k = 1.4458$ and $\lambda = 0.8428$. Notice that since we try to build a single model (not subject based), we estimate these single values for all the subjects.

The next step here is to modify the s values according to the Power Law model. These values then serve as the expected speed multipliers (i.e., ground truths) in our tests and we denote them as s_{exp}. Assuming a Power Law model version of Equation (1), the computation turns into:

$$\mathbf{v}_t = k \cdot (\mathbf{v}_r \cdot s_{exp})^{\lambda}$$
$$s_{exp} = \left(\frac{\mathbf{v}_t}{k \cdot \mathbf{v}_r^{\lambda}}\right)^{\frac{1}{\lambda}}.$$

After plugging in the k and λ values and performing the computations we find the estimation errors as

$$s_{err} = s_s - s_{exp}.$$

After the new error distribution is computed, we perform the analysis detailed in Section 5.2. As a companion to the discussions in that section, refer to Fig. 9 that displays the distribution of error values versus the global scale test parameter.

Acknowledgements

This work has been carried out within the VERDIKT funded project IllustraSound (# 193170) with support of the MedViz network in Bergen, Norway (PK1760-5897-Project 11). In addition, this work has been supported by Vienna Science and Technology Fund (WWTF) through project VRG11-010 and by EC Marie Curie Career Integration Grant through project PCIG13-GA-2013-618680. The authors would like to express their appreciation for the feedback from experts in visual perception and psychophysics. In particular, they would like to thank Prof. Jan Koenderink, who has encouraged them in the way how they pursued the research for obtaining the motion compensation model. Furthermore, they would like to thank the anonymous reviewers, who have pointed them to relevant psychophysics literature on

perceptual models, LCD and CRT screen particulars, and other suggestions that have helped them how to substantially improve the manuscript.

References

[1] H.-C. Nothdurft, "The role of features in preattentive vision: Comparison of orientation, motion and color cues," *Vis. Res.*, vol. 33, no. 14, pp. 1937–1958, 1993.

[2] B. Tversky, J. B. Morrison, and M. Betrancourt, "Animation: Can it facilitate?" *Int. J. Human-Comput. Stud.*, vol. 57, no. 4, pp. 247–262, 2002.

[3] I. Abbott and A. Von Doenhoff, *Theory of Wing Sections: Including a Summary of Airfoil Data*, Series Dover Books on Physics and Chemistry, New York, NY, USA: Dover, 1959.

[4] D. Acevedo, C. D. Jackson, F. Drury, and D. H. Laidlaw, "Using visual design experts in critique-based evaluation of 2D vector visualization methods," *IEEE Trans. Vis. Comput. Graph.*, vol. 14, no. 4, pp. 877–884, Jul. 2008.

[5] R. van Pelt, J. O. Bescos, M. Breeuwer, R. E. Clough, M. Eduard Groller, B. T. H. Romeny, and A. Vilanova, "Exploration of 4D MRI blood flow using stylistic visualization," *IEEE Trans. Vis. Comput. Graph.*, vol. 16, no. 6, pp. 1339–1347, Nov./Dec. 2010.

[6] R. van Pelt, J. Oliván Bescós, M. Breeuwer, R. E. Clough, M. Eduard Grø"ller, B. ter Haar Romeny, and A. Vilanova, "Interactive virtual probing of 4D MRI blood-flow," *IEEE Trans. Vis. Comput. Graph.*, vol. 17, no. 12, pp. 2153–2162, Dec. 2011.

[7] R. van Pelt, S. Jacobs, B. ter Haar Romeny, and A. Vilanova, "Visualization of 4D blood-flow fields by spatiotemporal hierarchical clustering," *Comput. Graph. Forum*, vol. 31, no. 3, pp. 1065–1074, 2012.

[8] W. Reichardt, "Autocorrelation, a principle for the evaluation of sensory information by the central nervous system," in *Principles of Sensory Communications*, 1961, pp. 303–317.

[9] J. P. Frisby and J. V. Stone, *Seeing: The Computational Approach to Biological Vision*, 2nd ed., Cambridge, MA, USA : MIT Press, 2010.

[10] P. Thompson, "Perceived rate of movement depends on contrast," *Vis. Res.*, vol. 22, no. 3, pp. 377–380, 1982.

[11] L. S. Stone and P. Thompson, "Human speed perception is contrast dependent," *Vis. Res.*, vol. 32, no. 8, pp. 1535–1549, 1992.

[12] M. R. Blakemore and R. J. Snowden, "The effect of contrast upon perceived speed: A general phenomenon?" *Perception*, vol. 28, no. 3, pp. 33–48, 1999.

[13] P. Thompson, K. Brooks, and S. T. Hammett, "Speed can go up as well as down at low contrast: Implications for models of motion perception," *Vis. Res.*, vol. 46, nos. 6/7, pp. 782–786, 2006.

[14] G. Mather, "Luminance change generates apparent movement: Implications for models of directional specificity in the human visual system," *Vis. Res.*, vol. 24, no. 10, pp. 1399–1405, 1984.

[15] A. Derrington and G. Henning, "Detecting and discriminating the direction of motion of luminance and colour gratings," *Vis. Res.*, vol. 33, nos. 5/6, pp. 799–811, 1993.

[16] P. Cavanagh, C. W. Tyler, and O. E. Favreau, "Perceived velocity of moving chromatic gratings," *J. Opt. Soc. Amer. A, Optics Image Sci.*, vol. 1, pp. 893–899, 1984.

[17] D. Weiskopf, "On the role of color in the perception of motion in animated visualizations," in *Proc. Conf. Vis.*, 2004, pp. 305–312.

[18] S. S. Stevens, "On the psychophysical law," *Psychol. Rev.*, vol. 64, no. 3, pp. 153–181, 1957.

[19] J. Ryan and J. Zanker, "What determines the perceived speed of dots moving within apertures?" *Exp. Brain Res.*, vol. 141, no. 1, pp. 79–87, 2001.

[20] J. Zanker, "Does motion perception follow Weber's law?" *Perception*, vol. 24, pp. 363–372, 1995.

[21] K. A. Turano and S. M. Heidenreich, "Speed discrimination of distal stimuli during smooth pursuit eye motion," *Vis. Res.*, vol. 36, no. 21, pp. 3507–3517, 1996.

[22] D. Regan, S. J. Hamstra, S. Kaushal, A. Vincent, and R. Gray, "Visual processing of the motion of an object in three dimensions for a stationary or a moving observer," *Perception*, vol. 24, pp. 87–103, 1995.

[23] S. Grossberg and M. E. Rudd, "Cortical dynamics of visual motion perception: Short-range and long-range apparent motion," *Psychol. Rev.*, vol. 99, no. 1, pp. 78–121, 1992.

[24] V. Šolteszova, C. Turkay, M. C. Price, and I. Viola, "A perceptual-statistics shading model," *IEEE Trans. Vis. Comput. Graph.*, vol. 18, no. 12, pp. 2265–2274, Dec. 2012.

[25] M. Gleicher, D. Albers, R. Walker, I. Jusufi, C. D. Hansen, and J. C. Roberts, "Visual comparison for information visualization," *Inf. Vis.*, vol. 10, no. 4, pp. 289–309, 2011.

[26] B. J. Geesaman and N. Qian, "A novel speed illusion involving expansion and rotation patterns," *Vis. Res.*, vol. 36, no. 20, pp. 3281–3292, 1996.

[27] S. N. Watamaniuk, N. M. Grzywacz, and A. L. Yuille, "Dependence of speed and direction perception on cinematogram dot density," *Vis. Res.*, vol. 33, nos. 5/6, pp. 849–859, 1993.

[28] M. McCool and E. Fiume, "Hierarchical poisson disk sampling distributions," in *Proc. Conf. Graph. Interface*, 1992, vol. 92, pp. 94–105.

[29] P. Wang and D. Nikolic, "An LCD monitor with sufficiently precise timing for research in vision," *Frontiers Human Neurosci.*, vol. 5, no. 85, 2011.

[30] F. A. Verstraten, "On the ancient history of the direction of the motion aftereffect," *Perception*, vol. 25, no. 10, pp. 1177–1187, 1996.

[31] N. J. Nagelkerke, "A note on a general definition of the coefficient of determination," *Biometrika*, vol. 78, no. 3, pp. 691–692, 1991.

Åsmund Birkeland received the PhD degree in informatics from the University of Bergen, Norway, in 2013. His research interests include medical visualization, perception, and image processing. He is a member of the IEEE.

Cagatay Turkay received the MSc degree from Sabanci University, Istanbul, Turkey, and the PhD degree from the University of Bergen, Norway. He is a faculty member and lecturer of applied data science at the gi-Centre at the Department of Computer Science at City University London, United Kingdom. His research interests mainly include the tight integration of interactive visualizations, data analysis techniques, and supporting exploratory knowledge and capabilities of experts. He has a special interest in high-dimensional, temporal data from bioinformatics and the biomolecular modelling domain.

Ivan Viola received the Dipl-Ing and Dr techn degrees from the Vienna University of Technology, Austria, in 2002 and 2005, respectively. He is an assistant professor at the Vienna University of Technology, Austria, and an adjunct professor at the University of Bergen, Norway. His research interests include illustrative visualization, which stands for new visual abstraction methods that are easy to interpret by humans from the perceptual and cognitive point of view, and are related to techniques developed in visual communication and arts. He coauthored several scientific works published in international journals and conferences such as *IEEE Transactions on Visualization and Computer Graphics*, IEEE Vis, EG CGF, and EG EuroVis, and acted as a reviewer and IPC member for conferences in the field of computer graphics and visualization. He is member of the IEEE Computer Society, Eurographics, VGTC, and the ACM.